# REPORT DOCUMENTATION PAGE

*Form Approved*
*OMB No. 0704-0188*



**PLEASE DO NOT RETURN YOUR FORM TO THE ABOVE ORGANIZATION.**

| 1. REPORT DATE *(DD-MM-YYYY)* | 2. REPORT TYPE | 3. DATES COVERED *(From - To)* |
|---|---|---|
| 02-29-2012 | Final Progress Report | 01/01/2009-11/30/2011 |

**4. TITLE AND SUBTITLE**
"From Ignition to Photoelectron Spectroscopy Conical Intersections Impact the Study of Energetic Materials"

**5a. CONTRACT NUMBER**

**5b. GRANT NUMBER**
FA9550-09-1-0038

**5c. PROGRAM ELEMENT NUMBER**

**6. AUTHOR(S)**
Yarkony, David, R,

**5d. PROJECT NUMBER**

**5e. TASK NUMBER**

**5f. WORK UNIT NUMBER**

**7. PERFORMING ORGANIZATION NAME(S) AND ADDRESS(ES)**
Johns Hopkins University
3400 N. Charles St.
W400 Wyman Park Bldg
Baltimore, MD 21218-2680

**8. PERFORMING ORGANIZATION REPORT NUMBER**
104843/90036446

**9. SPONSORING/MONITORING AGENCY NAME(S) AND ADDRESS(ES)**
Air Force Office of Scientific Research
875 N. Randolph St., Room 3112
Arlington, VA 22203

**10. SPONSOR/MONITOR'S ACRONYM(S)**
AFOSR

**11. SPONSOR/MONITOR'S REPORT NUMBER(S)**

**12. DISTRIBUTION/AVAILABILITY STATEMENT**

**13. SUPPLEMENTARY NOTES**

**14. ABSTRACT**

During the course of this grant improved algorithms for simulating photoelectron spectra were developed and used to simulate the photoelectron spectra of the cyclopentadienyl (CH)5 substitutional isomers triazolyl (CH)2N3 and pyrrolyl (CH)4N. The programmatic significance of this task lies in the importance of the parent azoles, (CH)nN(5-n)H, and their deprotonated counterparts, the azolides, as fundamental units in ionic liquids, explosives and fuels. Significant progress was also made in a study of the nonadiabatic photodissociation of furazan, (CH)2N2O ,another five member ring species. Furazan-based, high nitrogen content energetic materials have recently received significant attention for applications as explosives, fuels, and propellants due to their good heat resistivity, high heat of formation, low sensitivity, and good detonation performance. For these furazan based materials photo-induced dissociation of the electronically excited species is relevant to their denotation.

**15. SUBJECT TERMS**

| 16. SECURITY CLASSIFICATION OF: | | | 17. LIMITATION OF ABSTRACT | 18. NUMBER OF PAGES | 19a. NAME OF RESPONSIBLE PERSON |
|---|---|---|---|---|---|
| a. REPORT | b. ABSTRACT | c. THIS PAGE | SAR | | David R. Yarkony |
| | | | | | 19b. TELEPHONE NUMBER *(Include area code)* 410 516-4663 |

## INSTRUCTIONS FOR COMPLETING SF 298

**1. REPORT DATE.** Full publication date, including day, month, if available. Must cite at least the year and be Year 2000 compliant, e.g. 30-06-1998; xx-06-1998; xx-xx-1998.

**2. REPORT TYPE.** State the type of report, such as final, technical, interim, memorandum, master's thesis, progress, quarterly, research, special, group study, etc.

**3. DATES COVERED.** Indicate the time during which the work was performed and the report was written, e.g., Jun 1997 - Jun 1998; 1-10 Jun 1996; May - Nov 1998; Nov 1998.

**4. TITLE.** Enter title and subtitle with volume number and part number, if applicable. On classified documents, enter the title classification in parentheses.

**5a. CONTRACT NUMBER.** Enter all contract numbers as they appear in the report, e.g. F33615-86-C-5169.

**5b. GRANT NUMBER.** Enter all grant numbers as they appear in the report, e.g. AFOSR-82-1234.

**5c. PROGRAM ELEMENT NUMBER.** Enter all program element numbers as they appear in the report, e.g. 61101A.

**5d. PROJECT NUMBER.** Enter all project numbers as they appear in the report, e.g. 1F665702D1257; ILIR.

**5e. TASK NUMBER.** Enter all task numbers as they appear in the report, e.g. 05; RF0330201; T4112.

**5f. WORK UNIT NUMBER.** Enter all work unit numbers as they appear in the report, e.g. 001; AFAPL30480105.

**6. AUTHOR(S).** Enter name(s) of person(s) responsible for writing the report, performing the research, or credited with the content of the report. The form of entry is the last name, first name, middle initial, and additional qualifiers separated by commas, e.g. Smith, Richard, J, Jr.

**7. PERFORMING ORGANIZATION NAME(S) AND ADDRESS(ES).** Self-explanatory.

**8. PERFORMING ORGANIZATION REPORT NUMBER.** Enter all unique alphanumeric report numbers assigned by the performing organization, e.g. BRL-1234; AFWL-TR-85-4017-Vol-21-PT-2.

**9. SPONSORING/MONITORING AGENCY NAME(S) AND ADDRESS(ES).** Enter the name and address of the organization(s) financially responsible for and monitoring the work.

**10. SPONSOR/MONITOR'S ACRONYM(S).** Enter, if available, e.g. BRL, ARDEC, NADC.

**11. SPONSOR/MONITOR'S REPORT NUMBER(S).** Enter report number as assigned by the sponsoring/ monitoring agency, if available, e.g. BRL-TR-829; -215.

**12. DISTRIBUTION/AVAILABILITY STATEMENT.** Use agency-mandated availability statements to indicate the public availability or distribution limitations of the report. If additional limitations/ restrictions or special markings are indicated, follow agency authorization procedures, e.g. RD/FRD, PROPIN, ITAR, etc. Include copyright information.

**13. SUPPLEMENTARY NOTES.** Enter information not included elsewhere such as: prepared in cooperation with; translation of; report supersedes; old edition number, etc.

**14. ABSTRACT.** A brief (approximately 200 words) factual summary of the most significant information.

**15. SUBJECT TERMS.** Key words or phrases identifying major concepts in the report.

**16. SECURITY CLASSIFICATION.** Enter security classification in accordance with security classification regulations, e.g. U, C, S, etc. If this form contains classified information, stamp classification level on the top and bottom of this page.

**17. LIMITATION OF ABSTRACT.** This block must be completed to assign a distribution limitation to the abstract. Enter UU (Unclassified Unlimited) or SAR (Same as Report). An entry in this block is necessary if the abstract is to be limited.

**AEROSPACE, CHEMICAL AND MATERIAL SCIENCES DIRECTORATE**
**THEORETICAL CHEMISTRY AND MOLECULAR DYNAMICS**

**GRANT NUMBER: FA9550-09-1-0038**
**FINAL REPORT:**
**TITLE:FROM IGNITION TO PHOTOELECTRON SPECTROSCOPY CONICAL INTERSECTIONS IMPACT THE STUDY OF ENERGETIC MATERIALS**
**PRINCIPAL INVESTIGATOR: DAVID R. YARKONY, DEPARTMENT OF CHEMISTRY, JOHNS HOPKINS UNIVERSITY**

**PROGRAM MANAGER: DR. MICHAEL BERMAN**

## ABSTRACT

During the course of this grant improved algorithms for simulating photoelectron spectra were developed and used to simulate the photoelectron spectra of the cyclopentadienyl $(CH)_5$ substitutional isomers triazolyl $(CH)_2N_3$ and pyrrolyl $(CH)_4N$. The programmatic significance of this task lies in the importance of the parent azoles, $(CH)_nN_{5-n}H$, and their deprotonated counterparts, the azolides, as fundamental units in ionic liquids, explosives and fuels. Significant progress was also made in a study of the nonadiabatic photodissociation of furazan, $(CH)_2N_2O$ another five member ring species. Furazan-based, high nitrogen content energetic materials have recently received significant attention for applications as explosives, fuels, and propellants due to their good heat resistivity, high heat of formation, low sensitivity, and good detonation performance. For these furazan based materials photo-induced dissociation of the electronically excited species is relevant to their denotation.

## NARRATIVE

### I. Overview

The principal task we have addressed in the course of this grant is the determination of the negative ion photoelectron spectra of azolides, precursor anions to the azolyls, nitrogen heterocycles of the form $(CH)_{5-n}N_n$, $1 \le n \le 5$, whose vibronic spectra are observed in the experiment, azolide + $h\nu$ —> azolyl + $e^-$. The programmatic significance of this task lies in the importance of the parent azoles, $(CH)_nN_{5-n}H$, and their deprotonated counterparts, the azolides, as fundamental units in ionic liquids,[1,2] explosives[3] and fuels.[4] The thermochemistry of these azoles and negative ion photoelectron spectra of the azolides, have been reported by Lineberger's group at the University of Colorado.[5-8] The photoelectron spectra are quite complicated and most are poorly described by adiabatic techniques.[6,7,9] In order to carry out the simulations it was necessary to make significant upgrades[10,11] to the algorithms we had only recently developed[12-14] to describe nonadiabatic photoelectron spectra. The complexity is attributable to the existence of low-lying conical intersections of two and three electronic states which are not required by symmetry.[7,15,16] The existence of low-lying accidental three state conical intersections in these molecules, which was completely unprecedented, was established in the course of earlier AFOSR funded work.[15] The computational advances, and the computed spectra and their significance are described below.

Nonadiabatic photodissociation can play a role in detonation of energetic materials when the ignition processes involves sparks, shocks or laser heating.[17] We considered, in a project which is ongoing, the nonadiabatic photodissociation of furazan, $C_2H_2N_2O^* \rightarrow NO + C_2H_2N$. Our work brings new insights into a problem carefully studied experimentally and computationally in the laboratory of Bernstein[18] (Colorado State).

### II. Improved Algorithms for KDC Theory

A. An Enhanced Quadratic Vibronic Coupling Model-Existing Tools

The spectra computed during the course of this grant, those of pyrrolide and 1,2,3-triazolide, were to be computed using our second order implementation of the multimode vibronic model of Köppel, Domcke and Cederbaum(KDC Theory), [19,20] introduced 30 years ago and extended and improved since then by both those workers[21-24] and others.[7,12-14,25] In KDC theory, the computation of the photoelectron spectrum proceeds in two steps. In this presentation we use the language of negative ion photodetachment, although the approach is also suitable for photoionization. In the first step the $N^{state}$ coupled adiabatic electronic states of the neutral are described using a coupled quasi-diabatic state Hamiltonian, $\mathbf{H}^d$, constructed in $N^{int}$ nonredundant internal coordinates, $\mathbf{Q}$

$$H^d_{i,j}(\mathbf{Q}) = < \Psi^{e,d}_i(\mathbf{r}^{N^{el}},\mathbf{Q}) \mid H^{e,N^{el}} \mid \Psi^{e,d}_j(\mathbf{r}^{N^{el}},\mathbf{Q}) > = E^a_i(\mathbf{Q}^0)\delta_{i,j} + \sum_k V^{(1)i,j}_k Q_k + 1/2 \sum_{k,m} V^{(2)i,j}_{k,m} Q_k Q_m \quad (1)$$

where $1 \le i \le j \le N^{\text{state}}$, $\Psi^{e,d}_i$ is a quasi-diabatic electronic state, the coordinates of the $N^{el}$ electrons are denoted $\mathbf{r}^{N^{el}} = (\mathbf{r}_1, \mathbf{r}_2, \ldots . \mathbf{r}_{N^{el}})$ and $E^a_J$ is the adiabatic energy of the $J^{\text{th}}$ state. Note that $\mathbf{H}^d$ contains terms through second order in $\mathbf{Q}$, and the resulting KDC method is denoted the quadratic vibronic coupling (QVC) model. In our extension of the KDC-QVC method, $\Psi^{e,d}_i$ is not explicitly determined but rather the $\mathbf{V}^{(i)}$ are determined by requiring the adiabatic energies, energy gradients and derivative couplings obtained from $\mathbf{H}^d$ to reproduce, as well as possible, the

corresponding *ab initio* data. The unique aspect of our approach is that derivative coupling information is used in the construction of $\mathbf{H}^{\mathrm{d}}$. This results in a representation which is quantifiably quasi-diabatic in a least squares sense.[13]

In the second step, the total vibronic Schrödinger equation

$$(H^T - E_J^T)\Psi_J^T = 0 \tag{2a}$$

where $H^T = T^{\mathrm{nuc}} + H^{e,N^{el}}$, and $T^{nuc}$ is the nuclear kinetic energy operator, is solved. The eigenstates are expanded in a vibronic basis

$$\Psi_K^T(\mathbf{r}^{N^{el}},\mathbf{Q}) = \sum_{i=1}^{N^{state}} \Psi_i^{e,d}(\mathbf{r}^{N^{el}};\mathbf{Q}) \sum_{\mathbf{n}} c_{\mathbf{n}}^{K,i} \mid \mathbf{n} > \tag{2b}$$

where the vibrational basis, $|\mathbf{n}>$, is given in the multimode representation by[24]

$$\left|\mathbf{n}(\mathbf{Q})\right\rangle = \prod_{i=1}^{N^{\mathrm{int}}} \chi_{n_i}^{i}(Q_i) \qquad \text{for } 0 \le n_i < M_i \tag{2c}$$

and $\chi_n^i$ is the $n^{\mathrm{th}}$ harmonic oscillator function for the $i^{\mathrm{th}}$ mode of the neutral. In this basis eq. (2a) becomes:

$$\left[\mathbf{H}^T - E_K^T\mathbf{I}\right]\mathbf{c}^K = \mathbf{0} \tag{3a}$$

where

$$H^T_{i,\mathbf{n},j,\mathbf{m}} = \left\langle \mathbf{n} \mid T^{nuc}\delta_{i,j} + H^d_{i,j} \mid \mathbf{m} \right\rangle_{\mathbf{Q}} \quad . \tag{3b}$$

The multimode vibronic basis has dimension

$$N^{MM} = N^{state}N^{vib} \quad \text{where} \quad N^{vib} = \prod_{i=1}^{N^{\mathrm{int}}} M_i \tag{4}$$

which can easily exceed a billion terms, depending on the choice of $M_i$. However given the polynomial form of $\mathbf{H}^{\mathrm{d}}$ and harmonic oscillator products in $\mathbf{n}(\mathbf{Q})$, $\mathbf{H}^{\mathrm{T}}$ has structured sparsity.[24] The number of nonzero elements grows only linearly[14] with $N^{MM}$ and the location of the zeros in $\mathbf{H}^T$ is readily identified. $\mathbf{c}^K$ is determined from eq. (3a) using a Lanczos based "diagonalization."[26] As part of an earlier AFOSR grant, we developed[14] an open-ended fine-grained parallel Lanczos algorithm, which partitions the $N^{MM}$ dimensional vector, $\mathbf{c}^K$ among $N^{\mathrm{proc}}$ processors. This both reduces the time to solution of eq. (3a) and increases the maximum $N^{MM}$ which is practical. As currently implemented we can handle $N^{MM} \sim 10^{10}$, which is one to two orders of magnitude larger than that possible with single processor codes.

The simulated photoelectron spectrum is given by the spectral intensity distribution function, $P(E)$ where

$$P(E) = 2\pi \sum_K |B_K|^2 \, \delta(E - (E_K^T - E_0)) \quad \text{where} \quad B_K = \left\langle \hat{\mu}\Psi_0^T \middle| \Psi_K^T \right\rangle \quad . \tag{5}$$

Here, $\hat{\mu}$ is a many electron dipole moment operator, $\Psi_0^T$ is the vibronic wave function of the negative ion which is assumed to be in its ground vibrational level and well described in the adiabatic state-harmonic oscillator (the quadratic, adiabatic) approximation, that is

$$\Psi_0^T(\mathbf{r}^{N^{el}+1},\overline{\mathbf{Q}}) = \Psi_0^{a,an}(\mathbf{r}^{N^{el}+1};\overline{\mathbf{Q}}) \mid \overline{\mathbf{0}} > = \Psi_0^{a,an}(\mathbf{r}^{N^{el}+1};\overline{\mathbf{Q}}) \sum_{\mathbf{n}} c_{0,\mathbf{n}}^{\mathbf{0}} \mid \mathbf{n} > \tag{6a}$$

where $\Psi_0^{a,an}(\mathbf{r}^{N^{el}+1};\overline{\mathbf{Q}})$ is the ground adiabatic electronic state of the anion, $\left|\overline{\mathbf{0}}\right\rangle$ denotes the ground vibrational level, the overbar indicates that the vibrational coordinates and harmonic oscillator functions, are appropriate for the anion or precursor molecule and may differ from

those of the neutral. The $c^{\mathbf{0}}_{0,\mathbf{m}}$ are multidimensional Franck-Condon factors

$$c^{\mathbf{0}}_{0,\mathbf{m}} = <\bar{\mathbf{0}}\,|\,\mathbf{m}> \quad \text{where } \langle\bar{\mathbf{n}}|\mathbf{m}\rangle = \left\langle \prod_{i=1}^{N^{\rm int}} \bar{\chi}^{i}_{n_i}(\bar{Q}_i) \middle| \prod_{i=1}^{N^{\rm int}} \chi^{i}_{m_i}(Q_i) \right\rangle \quad . \tag{6b}$$

The spectral intensity, $|B_K|^2$ for the transition from the ground level of the negative ion, given by eq, (6a), to the $K^{\rm th}$ state of the neutral, given by eqs. (2b, 2c) is readily shown to be:[12]

$$B_K = \sum_{j=1}^{N^{state}} \sum_{\mathbf{m},\mathbf{n}} c^{\mathbf{0}}_{0,\mathbf{m}} \boldsymbol{\mu}^{0,j}_{\mathbf{m},\mathbf{n}} c^{K}_{j,\mathbf{n}} \approx \sum_{j=1}^{N^{state}} \sum_{\mathbf{n}} (\mu_{0,j} c^{\mathbf{0}}_{0,\mathbf{n}}) c^{K}_{j,\mathbf{n}} \tag{7}$$

where

$$\boldsymbol{\mu}^{0,j}_{\mathbf{m},\mathbf{n}} = \langle \mathbf{m} | \mu_{0,j} | \mathbf{n} \rangle_{\mathbf{Q}} \approx \mu_{0,j} \delta_{\mathbf{m},\mathbf{n}} \tag{8a}$$

$$\mu_{0,j}(\mathbf{Q}) = \left\langle \Psi^{a,an}_{0}(\mathbf{r}^{N^{el}+1};\mathbf{Q}) | \hat{\mu} | \sum_{j=1}^{N^{state}} \Psi^{d,n}_{j}(\mathbf{r}^{N^{el}};\mathbf{Q}) \right\rangle_{\mathbf{r}} \quad . \tag{8b}$$

The $c^{K}_{j,\mathbf{n}}$ are obtained from eq. (3a) using the open-ended Lanczos algorithm. The second equality in eq. (7) or (8a) is valid when the **Q** dependence of $\mu_{0,j}(\mathbf{Q})$ can be neglected. $B_K$ can be determined without explicit determination of $c^{K}_{j,\mathbf{n}}$ if the seed vector in the Lanczos procedure is properly chosen.[7,12,24]

We also showed[12] that with a judicious choice of the $\chi^{i}_{m}$ (eq. 2c), $N^{MM}$ can be reduced considerably, by factors of 30 to 300 in our test case,[12] further extending the range of problems that can be treated. In order to exploit this basis set flexibility the Franck-Condon factors in eq. (6b) are required. We developed[12] an algorithm which uses fine grained parallelism to efficiently and exactly determine the millions to billions of multidimensional Franck-Condon overlap integrals.[19,27-31].

The electronic transition dipole moment in eq. (8b) deserves further comment. Note that, eq. (8b) is significantly oversimplified, since the anion wave function contains $N^{el}$+1 electrons while that of the neutral contains only $N^{el}$ electrons. The discrepancy is attributable to the failure to incorporate a description the detached electron. This issue is addressed in the research proposal submitted as the renewal of this grant.

**B. Higher order contributions to $\mathbf{H}^{\rm d}$**

As discussed below, the QVC model described above, currently the workhorse of the field,[24] worked quite well for the photoelectron spectrum of pyrrolide [ $(CH)_4N^-$ ] but proved inadequate for the description of the spectrum of triazolide [ $(CH)_2N_3^-$ ]. Consequently during the current performance period, the domain of utility and the accuracy of $\mathbf{H}^{d}$ were extended by including higher order terms.[11] Our $\mathbf{H}^{\rm d}$, through fourth order, is given by

$$H^{d}_{\alpha,\beta} - [E^{a}_{\alpha}\delta_{\alpha,\beta} + \sum_{k} V^{(1),\alpha,\beta}_{k} Q_k + 1/2 \sum_{k,m} V^{(2),\alpha,\beta}_{k,m} Q_k Q_m] = H^{d,(3,4)}_{\alpha,\beta}(\mathbf{Q}) \tag{9a}$$

$$H^{d,(3,4)}_{\alpha,\beta}(\mathbf{Q}) = \frac{1}{3!} \sum_{k,l,m=1}^{N^{\rm int}} V^{(3),\alpha,\beta}_{k,l,m} Q_k Q_l Q_m + \frac{1}{4!} \sum_{j,k,l,m=1}^{N^{\rm int}} V^{(4),\alpha,\beta}_{j,k,l,m} Q_j Q_k Q_l Q_m \tag{9b}$$

The algorithm, to determine this $\mathbf{H}^{\rm d}$ has been discussed in detail in Ref. [11]. Unlike other implementations of higher order terms,[32,33] our implementation, does not require the simplifications due to high symmetry. As with the $\mathbf{H}^{\rm d}$ in eq. (1) this representation is

quantifiably quasi-diabatic in a least squares sense.[11]

Our simulation of the triazolide spectrum described below[10] which required $\boldsymbol{V}$ through 4th order, provided insights into the need for higher order terms. The fourth order terms were required, not because $N^{state} = 4$ was needed, for the other azolyls treated $N^{state} = 2$ (Refs. [16,34]) or 3 (Refs. [7,35]) had been adequate but rather because of the comparatively large geometrical separation of key features of the adiabatic potential energy surfaces, minima, transition states and conical intersection seams.[11]

**C. A general open-ended Lanczos procedure for $\mathbf{H}^d$ with Higher Order Terms.**

The polynomial form in eqs. (9a,9b) preserves the structured sparsity of $\mathbf{H}^T$ in eq. (3a). As part of our AFOSR funded research,[10] we used this property to develop a fine-grained parallel version of the Lanczos "diagonalization" algorithm that can handle arbitrary $\mathbf{V}^{(n)}$ contributions. This algorithm, which is now in routine use, allows us to exploit the enhanced capability of the higher order $\mathbf{H}^d$ to achieve accurate simulations in computationally challenging systems.

**III. Azolide Photoelectron Spectra.**

We now turn to the results of the simulations of the azolide photoelectron spectra which reveal the spectra of the azolyls. The $(CH)_mN_{5-m}^-$ heterocycle anions are of programmatic interest as potential anionic components of ionic liquids and as tools to infer properties of pentaazolide, $N_5^-$.[9,36] The thermodynamics of these anions was studied both experimentally and computationally by Lineberger's group at the University of Colorado.[5-8,37,38]

The azolyls are substitutional isomers of the $D_{5h}$ cyclodentadienyl radical, $(CH)_5$ whose $^2E_1''$ ground state is Jahn-Teller distorted.[39-41] Replacing CH groups with N atoms both reduces the point group to $C_{2v}$ and introduces in-plane lone pair orbitals, excitations from which lead to low-lying excited states. The $^2E_1''$ symmetry-required conical intersection seam in cyclopentadienyl becomes a symmetry-allowed seam in an azolyl and the additional low-lying excited states can lead to additional conical intersection seams. Since our enhanced QVC algorithms, discussed in Section IIA, had previously enabled us to determine the photoelectron spectrum of the pyrazolide – pyrazolyl system $[(CH)_3N_2]$ (Ref. [35]) which had, at that time, been declared 'noncomputable' using, then state of the art time-independent QVC techniques,[7] we expected the nonadiabatic pyrrolide and triazolide simulations to be readily amenable to our QVC treatment. This did not turn out to be the case.

**A. Photoelectron spectrum of the pyrrolide-pyrrolyl system:** 

The most acidic site on pyrrole, $C_4NH_5$ is the nitrogen.[9] Deprotonation at this site produces the anion pyrrolide, $(CH_4)N^-$, whose photoelectron spectrum reveals the vibronic spectrum of pyrrolyl. In pyrrolyl, pictured above, the $^2E_1''$ ground state of cyclopentadienyl is split into a $^2A_2$ ground state and a $^2B_1$ excited state. The symmetry-required $^2E_1''$ conical intersection seam in cyclopentadienyl becomes a symmetry-allowed $^2A_2 - {}^2B_1$ accidental seam of conical intersection, whose minimum energy crossing point is 4436 $cm^{-1}$ above the $^2A_2$ ground state minimum.[34] The minimum energy $C_{2v}$ nuclear configuration where the wave function carries a $^2B_1$ irreducible representation is a saddle point. Fig.1 presents the pyrrolide photoelectron spectra determined experimentally[9] and simulated[34] using our nonadiabatic two state QVC method. Domcke and coworkers[16] have also reported a nonadiabatic simulation.

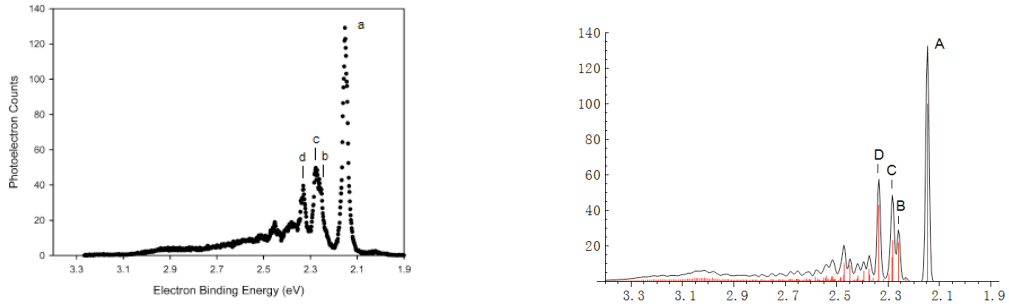


(a) (b)

Figure 1: Pyrrolide photoelectron spectrum. (a)Experimentally measured[9] (b)Computed nonadiabatic simulation[34]

From this figure is seen that when the electron binding energy (eBE) is less than ~ 2.4 eV the agreement between theory and experiment is quite good. Similar conclusions hold for a purely adiabatic determination of the photoelectron[9] spectrum based on the $^2A_2$ state. However, as originally noted in Ref. [9], attempts to include the effects of the $^2B_1$ state using an adiabatic approach produce "a prominent, well-resolved photoelectron spectrum beginning about 0.5 eV above the ground-state origin." But "no such spectrum is observed."[9] As discussed in Refs. [9] and [16] and confirmed by our calculations,[34] this a consequence of the nonadiabatic interactions induced by the $^2A_2 - {}^2B_1$ seam of conical intersection. This observation is not entirely surprising since, as noted above, the minimum energy conical intersection is ~0.55 eV (4436 $cm^{-1}$) above the ground state origin.

The good agreement of the intensities, peak heights, between the measured and our simulated spectrum for electron binding energy (eBE) > ~ 2.6 eV is a consequence of two factors: the inclusion of nonadiabatic interactions through $\mathbf{H}^d$ and; adjusting $r = \mu_{0,^2A_2} / \mu_{0,^2B_1}$ from the standard choice[24] $r = 1$, to $r = 2$. It was need for this empirical correction to the transition dipole moments that served to motivate the approximate first principles determination of $\mu_{0,j}$ discussed in our AFOSR renewal proposal.

A question of fundamental importance, which has received only limited attention,[42,43] is how far below the minimum energy crossing, are the effects of the conical intersection seam felt. Analysis of the vicinity of the peak labeled B in Fig. 1 at eBE 2.257 eV (905 $cm^{-1}$) evinces a shoulder at 2.229 eV, only 675 $cm^{-1}$, 0.084 eV, above threshold and ~3760 $cm^{-1}$ below the minimum energy crossing. A symmetry analysis of our wave functions shows that this shoulder, which is absent in the adiabatic simulation, is due to nonadiabatic coupling to the $^2B_1$ diabat. With the advent of high resolution SEVI and PFI-PE spectroscopy such low intensity peaks should be readily discerned. Given that the feature in question is ~3760 $cm^{-1}$ below the minimum energy crossing its nonadiabatic character is quite surprising. The extent of nonadiabatic intrusion into ostensibly adiabatic regions of photoelectron spectra is an important fundamental issue of practical import. This question will be addressed in our AFOSR renewal proposal.

**B. Photoelectron spectrum of the triazolide-triazolyl system:** 

The 1,2,3-triazolide anion, $(CH)_2N_3^-$, is obtained by deprotonaton of 1H-1,2,3-triazole at the most acidic site, the nitrogen atom. This system has been studied experimentally and

computationally in Lineberger's laboratory.[38] Lineberger observed that the experimental spectrum could not be simulated using a quadratic, adiabatic description of the neutral.[38] The failure of the quadratic, adiabatic description of 1,2,3-triazolyl was surprising in view of the fact that the minimum energy point on the conical intersection seam is 3737 $cm^{-1}$ (0.463 eV) above the ground state minimum.[10] In the case of pyrrolide we were able to identify small nonadiabatic effects in the experimental spectrum at energies that extend well below the minimum energy point on the conical intersection seam. Attempts to perform a similar analysis for 1,2,3-triazolide were complicated by the fact that the nonadiabatic effects lie in a spectral region where hot band sequences exist. Thus the simulation of photoelectron spectrum of 1,2,3- triazolide was particularly challenging since it required us to address a combination of issues.

Fig. 2 compares our nonadiabatic simulation, with the experimentally measured spectrum. The agreement is, as discussed in Ref. [10], quite reasonable. Below we discuss how, in general, this agreement was achieved, and the spectrum near peak A, the origin peak identified by Lineberger.

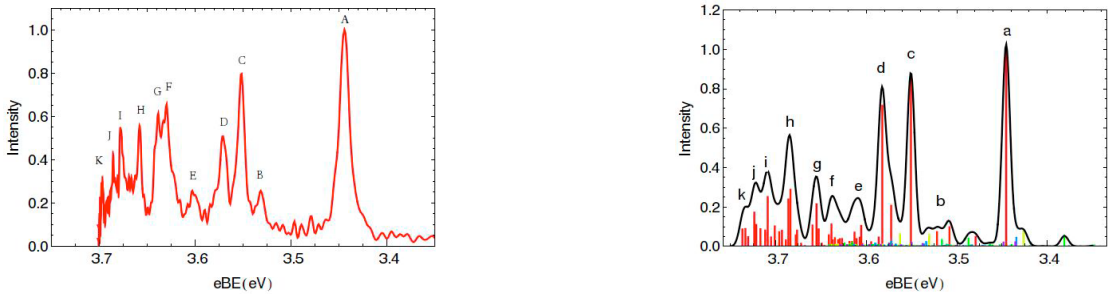


(a) (b)

Figure 2: Triazolide photoelectron spectrum. (a) Experimental spectrum.[38] (b). Simulation of based on $\mathbf{H}^{d}$ including $\mathbf{H}^{d,(3,4)}$. Contributions originating from five vibrational levels of the anion are included: ground state(red) , remainder have one phonon in $\omega_7$(purple), $\omega_8$(green), $\omega_9$(blue), and $\omega_{10}$(yellow), respectively.

The simulations of the ground state and hot band photoelectron spectra of 1,2,3-triazolide each required $N^{MM} \sim 10^9$. This simulation differed from our previous AFOSR sponsored simulations of pyrrolide[34] and pyrazolide[35] in two fundamental aspects. While pyrrolide required two states and pyrazolide required three states in the simulations, triazolide required four states to simulate. In addition while the quadratic vibronic coupling model performed admirably for pyrrolide and pyrazolide, the fourth-order quasi-diabatic Hamiltonian, $\mathbf{H}^{d}$, discussed above, was required for triazolide. To carry out these calculations three algorithmic extensions were required, including the higher order $\mathbf{H}^{d}$ algorithm described in section IIB and the general open ended Lanczos algorithm described in section IIC. We also introduced into the Lanczos algorithm[10] the capability treat hot band spectra while reducing the size of the vibrational basis used in eq. (2). This required calculating Franck-Condon overlaps of the form $\langle \overline{\mathbf{m}}^{i} | \mathbf{n} \rangle$ where $|\overline{\mathbf{m}}^{i}\rangle$ is hot band state of the anion with one phonon excited, $\overline{m}^{i}_{j} = \delta_{i,j}$ and $\mathbf{n}>$ is given in eq. (2c). This extended our existing algorithm,[12] which was restricted to the vibrational ground state of the anion, that is $\overline{\mathbf{m}} = \mathbf{0}$.

For the triazolide photoelectron spectrum, the simulation based on the quartic $\mathbf{H}^{d}$ is far superior at reproducing the main features of the experimental spectrum, when compared with

standard quadratic $\mathbf{H}^{d}$ based simulation and allowed for the assignment of the main vibronic transitions observed in the experimental spectrum. Sequence (vibrationally excited anion) band contributions, corresponding to one quantum in each of four low frequency modes of the triazolide anion, explain the observed vibronic transitions occurring to the red of the assigned band origin of the neutral species and some weak transitions to the blue of the origin band. See Fig. 2 where color codingn is used to identify hot bands.

The peak labeled *b* occurring at ~3.500-3.525eV (~500-621 $cm^{-1}$ above threshold and ~3200-3100 $cm^{-1}$ below the minimum energy conical intersection), is relevant to the issue of nonadiabatic effects intruding into what would be expected to be adiabatic spectral regions. The peak labeled *b* is actually composed of two weak transitions, denoted *b*' and *b*". Such weak peaks are frequently assigned, as combination bands in the adiabatic approximation. However they can also be (nontotally symmetric) fundamentals of nonadiabatic transitions. In this example both situations are found. The *b*' eigenstate arises from nonadiabatic interactions while the principal contributor to the *b*" level is an overtone peak. Here assignments based solely on energy can be problematic owing to the practical limits of the frequencies obtained from *ab initio* calculations.

Thus, as in the case of pyrrolyl, nonadiabatic interactions are demonstrable well below the energies of the minimum energy conical intersection. However, under the experimental conditions, we also found that the size of the contributions from hot bands and weak adiabatic (allowed) transitions were comparable to those of the nonadiabatic transitions, complicating the experimental assignment of the observed transitions. As noted above the existence of nonadiabatic effects in photoelectron spectra in regions energetically well below the minimum energy conical intersection raised the question of the generality of this observation. This issue is addressed in our AFOSR renewal proposal.

## IV. Conical Intersections and Photo-induced Decomposition of Energetic Materials

### A. Furazan $(CH)_2N_2O$ 

Furazan-based, high nitrogen content energetic materials, especially DAAF (3,3′-diamino-4,4′-azoxyfurazan = two amino furazan rings joined by an azoxy group), have recently received significant attention for applications such as explosives, fuels, and propellants due to their good heat resistivity, high heat of formation, low sensitivity, and good detonation performance.[44] The basic unit of these materials furazan, pictured above, is a cyclopentadienyl ring with three CH groups replaced by two nitrogens and one oxygen. For these furazan based materials photo-induced dissociation of the electronically excited species is relevant to their denotation. Consequently the photodissociation of DAAF and related model systems including furazan itself have been studied both experimentally and computationally by Bernstein and coworkers.[44]

Our ongoing study of furazan photodissociation[45] builds on the experimental and computational work of Bernstein[18] and on the insights acquired in our studies of the azolides. Bernstein's experiments show that the initial product of the photodissociation is NO and that rotational energy in the NO fragment depends on the excitation wavelength. Bernstein attributed the differences in rotational energy in the products to the existence of distinct pathways through

different conical intersections. Our studies of photodissociation in systems such as $CH_2COH$ +hv → $CH_2CO$+H (Ref. [46,47]) revealed that *g-h plane routing* can also lead to different energy distributions in the products.

Numerical studies of the photodissociation of furazan are complicated by the fact that four states must be considered in the entrance channel – not unlike the situation in triazolyl - while only two, the states correlating with NO($^2\Pi$), must be considered in the product channel. To treat this properly we are implementing a generally weighted state averaged multiconfiguration self consistent field, GW-SA-MCSCF procedure.[48] The need to consider four states in the reaction channel is a consequence of the existence of two nitrogen atoms in furazan. This in turn suggests the possibility of three state conical intersections in the Franck-Condon (FC) region. Indeed in preliminary calculations a point of intersection of $S_1$, $S_2$ and $S_3$ has been located, which is only slightly (~2000 $cm^{-1}$) higher than the minimum on the $S_1$ potential energy surface. This three state intersection has a five dimensional branching space[49] which facilitates motion from the planar structures in the FC region to nonplanar structures.

Using multireference configuration interaction wave functions, we have located a low energy conical intersection similar to one determined by Bernstein. This intersection, Fig. (3a), is ~ 20,000 $cm^{-1}$ below the energy of the first excited state ($S_1$) in the Franck-Condon region and lower in energy than the azirene (Fig. (3c)) + NO asymptote Our ongoing analysis of molecular motion following an encounter with this conical intersection reflects *g-h* plane routing, Fig. (3a).

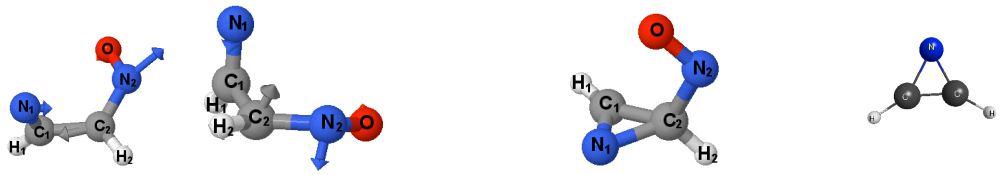


**g** (a) **h** (b) (c)

Figure 3 (a) Two views of the furazan low energy conical intersection, with **g** and **h** vectors superimposed respectively, (b) an intermediate, and (c) azirene a decomposition product $(CH)_2N$

As seen from the *g-h* plane in Fig. (3a), not considered in previous studies, both +**g** and ±**h** motion produce a torque on the NO moiety. We find motion starting along -**g** leads the local minimum structure pictured in Fig. (3b). Again this structure was not previously reported.

## References


1 Y. R. Jorapur, J. M. Jeong, and D. Y. Chui, Tetrahedron Lett. **47**, 2435 (2006).

2 W. Ogihara, M. Yoshizawa, and H. Ohno, Chem. Lett. **33**, 1022 (2004).

3 G. K. Williams, S. F. Palopoli, and T. B. Brill, Combust. Flame **98**, 197 (1994).

4 Y. Okumara, Y. Sugiyama, and K. Okazaki, Fuel **81**, 2317 (2002).

5 S. Kato, R. Hoenigman, A. Gianola, T. Ichino, V. Bierbaum, and W. C. Lineberger, in *Molecular Dynamics and Theoretical Chemistry Contractors Review*, edited by M. Berman (AFOSR, Shelter Point Hotel, San Diego, CA, 2003), pp. 49.

6 A. J. Gianola, T. Ichino, S. Kato, V. M. Bierbaum, and W. C. Lineberger, J. Phys. Chem. A **110**, 8457 (2006).

[7] T. Ichino, A. J. Gianola, W. C. Lineberger, and J. F. Stanton, J. Chem. Phys. **125**, 084312 (2006).

[8] S. M. Villano, A. J. Gianola, N. Eyet, T. Ichino, S. Kato, V. M. Bierbaum, and W. C. Lineberger, J. Phys. Chem. A **111**, 8579 (2007).

[9] A. J. Gianola, T. Ichino, R. L. Hoenigman, S. Kato, V. M. Bierbaum, and W. C. Lineberger, J. Phys. Chem. A **108**, 10326 (2004).

[10] J. Dillon, D. R. Yarkony, and M. S. Schuurman, J. Chem. Phys. **134**, 184314(13 pages) (2011).

[11] J. J. Dillon, D. R. Yarkony, and M. S. Schuurman, J. Chem. Phys. **134**, 044101 (11 pages) (2011).

[12] M. S. Schuurman and D. R. Yarkony, J. Chem. Phys. **128**, 044119(9 pages) (2008).

[13] B. N. Papas, M. S. Schuurman, and D. R. Yarkony, J. Chem. Phys. **129**, 124104(10 pages) (2008).

[14] M. S. Schuurman, R. A. Young, and D. R. Yarkony, Chem. Phys. **347**, 57 (2008).

[15] S. Matsika and D. R. Yarkony, J. Amer. Chem. Soc. **125**, 12428 (2003).

[16] A. Motzke, Z. Lan, C. Woywod, and W. Domcke, Chem. Phys. **329**, 50 (2006).

[17] E. R. Bernstein, in *Overviews of Recent Research on Energetic Materials*, edited by D. Thompson, T. Brill, and R. Shaw (World Scientific, Hackensack, NJ, 2004).

[18] Y. Guo, A. Bhattacharya, and E. R. Bernstein, J. Chem. Phys. **128**, 034303 (2008).

[19] L. S. Cederbaum and W. Domcke, J. Chem. Phys. **64**, 603 (1976).

[20] H. Köppel, L. S. Cederbaum, and W. Domcke, Chem. Phys. **69**, 175 (1982).

[21] H. Köppel, W. Domcke, and L. S. Cederbaum, Adv. Chem. Phys. **57**, 59 (1984).

[22] H. Köppel, L. S. Cederbaum, and W. Domcke, J. Chem. Phys. **89**, 2023 (1988).

[23] S. Mahapatra, G. A. Worth, H.-D. Meyer, L. S. Cederbaum, and H. Köppel, J. Phys. Chem. A **105**, 5567 (2001).

[24] H. Köppel, W. Domcke, and L. S. Cederbaum, in *Conical Intersections*, edited by W. Domcke, D. R. Yarkony, and H. Köppel (World Scientific, New Jersey, 2004), Vol. 15, pp. 323.

[25] M. Nooijen, Int. J. Quantum Chem. **95**, 768 (2003).

[26] W. Domcke, H. Köppel, and L. Cederbaum, Mol. Phys. **43**, 851 (1981).

[27] E. V. Doktorov, I. A. Malkin, and V. I. Man'ko, J. Mol. Spec. **56**, 1 (1975).

[28] E. V. Doktorov, I. A. Malkin, and V. I. Man'ko, J. Mol. Spec. **64**, 302 (1977).

[29] A. Warshel and M. Karplus, Chem. Phys. Lett. **17**, 7 (1972).

[30] A. Warshel and P. Dauber, J. Chem. Phys. **66**, 5477 (1977).

[31] D. J. Tannor and E. J. Heller, J. Chem. Phys. **77**, 202 (1982).

[32] A. Viel and W. Eisfeld, J. Chem. Phys. **120**, 4603 (2004).

[33] W. Eisfeld and A. Viel, J. Chem. Phys. **122**, 204317 (2005).

[34] X. Zhu and D. R. Yarkony, J. Phys. Chem. C **114**, 5312 (2010).

[35] M. S. Schuurman and D. R. Yarkony, J. Chem. Phys **129**, 064304(14 pages) (2008).

[36] S. Kato, J. Mass Spectrom. Soc Jpn **53**, 183 (2005).

[37] T. Ichino, A. J. Gianola, S. Kato, V. M. Bierbaum, and W. C. Lineberger, J. Phys. Chem. A **111**, 8374 (2007).

[38] T. Ichino, D. H. Andrews, G. J. Rathbone, F. Misaiozu, R. M. D. Calvi, S. W. Wren, S. Kato, V. M. Bierbaum, and W. C. Lineberger, J. Phys. Chem. B **112**, 545 (2008).

[39] B. E. Applegate, T. A. Miller, and T. A. Barckholtz, J. Chem. Phys. **114** (11), 4855 (2001).

[40] B. E. Applegate, A. J. Bezant, and T. A. Miller, J. Chem. Phys. **114** (11), 4869 (2001).

[41] T. Ichino, S. W. Wren, K. M. Vogelhuber, A. J. Gianola, W. C. Lineberger, and J. F. Stanton, J. Chem. Phys. **129**, 084310 (19 pages) (2008).

[42] K. M. Ervin and W. C. Lineberger, J. Phys. Chem. **95**, 1167 (1991).

[43] K. R. Asmis, T. R. Taylor, and D. M. Neumark, J. Chem. Phys. **111**, 8838 (1999).

[44] A. Bhattacharya, Y. Guo, and E. R. Bernstein, Accounts of Chem. Res. **43**, 1476 (2010).

[45] D. Rabli, D. R. Yarkony, and J. J. Dillon, work in progress (2012).

[46] B. C. Hoffman and D. R. Yarkony, J. Chem. Phys. **116**, 8300 (2002).

[47] D. R. Yarkony, J. Chem. Phys. **122**, 084316 (2005).

[48] R. Dawes, A. W. Jasper, C. Tao, C. Richmond, C. Mukarakate, S. H. Kable, and S. A. Reid, J. Pys. Chem. Lett. **1**, 641 (2010).

[49] S. Matsika and D. R. Yarkony, J. Chem. Phys. **117**, 6907 (2002).

**Publications from FA9550-09-1-0038**
Jan 1, 2009 – Nov. 30, 2011

1. *The Photoelectron Spectrum of Pyrrolide: Nonadiabatic effects due to Conical Intersections*
   Xiaolei Zhu and David R. Yarkony, J. Phys. Chem. C 114, 5312-5320 (2010)

2. *On the Construction of Quasi Diabatic State Representations of Bound Adiabatic State Potential Energy Surfaces Coupled by Conical Intersections. Incorporation of Higher Order Terms*
   Joseph J. Dillon, David R. Yarkony and Michael S. Schuurman, J. Chem. Phys. 134, 044101 (2011).

3. *On the Simulation Photoelectron Spectra Complicated by Conical Intersections:Higher-Order Effects and Hot Bands in the Photoelectron Spectrum of Triazolide* $(CH)_2N_3^-$
   Joseph Dillon, David R. Yarkony and Michael S. Schuurman, J. Chem. Phys. 134, 184314(13 pages) (2011)

**Personnel**

**Principal Investigator**
David R. Yarkony
Department of Chemistry
Johns Hopkins University

**Graduate Students**
Xiaolei Zhu
Department of Chemistry
Johns Hopkins University

**Posdoctoral Research Associates**
Joseph Dillon
Department of Chemistry
Johns Hopkins University

Djamal Rabli
Department of Chemistry
Johns Hopkins University